Journal of Nuclear Materials 516 (2019) 160–168

Contents lists available at ScienceDirect

Journal of Nuclear Materials

journal homepage: www.elsevier.com/locate/jnucmat

Corrosion protective action of different coatings for the helium cooled pebble bed breeder concept

T. Hernández [a, *], F.J. Sánchez [a], F. Di Fonzo [b], M. Vanazzi [b], M. Panizo [c], R. González-Arrabal [c]

[a] National Laboratory for Magnetic Fusion, CIEMAT Avda, Complutense 40, 28040, Madrid, Spain
[b] Center for Nano Science and Technology @PoliMi, Istituto Italiano di Tecnologia, IIT Via Giovanni Pascoli 70/3, 20133 Milan, Italy
[c] Instituto de Fusión Nuclear, ETSII, Universidad Politécnica de Madrid (UPM), C/José Gutiérrez Abascal, 2, 28006 Madrid, Spain

ARTICLE INFO

Article history:
Received 30 August 2018
Received in revised form
5 December 2018
Accepted 4 January 2019
Available online 8 January 2019

ABSTRACT

An additional function of the permeation barriers is the protective action against corrosion. Although corrosion is not expected to be a major concern for the helium cooled pebble bed concept, it is not negligible and the joint action of the working temperature (350ºC-550 °C) and the lithium ceramic pebbles produces a corrosion layer in the surface of Eurofer material directly exposed to this environment.

Accelerated corrosion tests have been carried out in Eurofer protected by different coatings including Al_2O_3 prepared by pulsed laser deposition and thermal projection, nano-structured tungsten prepared by DC magnetron sputtering and other commercial coatings based on mixed chromium and aluminum oxinitrides obtained by arc evaporation technique. Tests were performed using a mixture of He/H_2O as a purge gas.

Two different lithium ceramics pebbles were tested: lithium orthosilicate (K-S) prepared in KIT by the KALOS method and lithium metatitanate obtained by the emulsion method in JAEA (J-T).

This paper compares the corrosion layer produced at different temperatures (550 °C and 800 °C) and shows the protection provided by certain coatings under severe conditions of temperature (800 °C) for 730 h. The most promising results have been obtained for aluminum oxide coatings, which stands out this material as the best candidate.

1. Introduction

Corrosion problems in breeder blankets have always been associated with the helium cooled lithium lead (HCLL) and the dual coolant lithium lead (DCLL) breeder concepts for working with liquid metals [1] combined with magnetic fields [2]. However, recent studies have shown that also in the helium cooled pebble bed (HCPB) concept, solid state reactions occur between the ceramic lithium pebbles and the Eurofer giving rise to corrosion layers. Depending on the temperature conditions and purge gas, the corrosion layer formed may be important and should not be neglected. Traditionally, He + H_2 mixture has been preferred as a purge gas, because He + H_2O cause a significant corrosion in Eurofer and an exothermic reaction with beryllium pebbles, forming hydrogen [3]. It is known that the corrosion produced in Eurofer by lithium ceramics by mixture He + 0.1% H_2 to 623 K is very low, less than 1 micron after 1350 h of testing; however, this value grows exponentially with temperature [4]. In the last years, The HCPB concept has been established as one of the most promising and the progress in its problem has been relevant [5]. Thus, it was proposed to study not only He + H_2 as purge gas but also He + H_2O as an alternative to He + H_2 because water is a better tritium carrier than hydrogen. Anyway, even purging with He + H_2 there will be a certain percentage of tritium (less than 10%) that will be purged in the form of T_2O instead of HT and that therefore will also corrode the Eurofer. On the other hand, if the He + H_2O mixture is used, the isotopic exchange with tritium will produce HTO, which does not permeate the coolant. This can turn out to be a huge advantage for the HCPB concept [6].

In that sense, it is important to know the actual extent of the

* Corresponding author.
E-mail address: teresa.hernandez@ciemat.es (T. Hernández).

https://doi.org/10.1016/j.jnucmat.2019.01.009
0022-3115/

corrosion of the He/H_2O gas mixture and the capacity of certain coatings to reduce the effect. Previous works have described the corrosion produced in different atmospheres and in relevant fusion conditions of temperature (550 °C) and time (3700 h) [7,8]. Here, some information is provided on the capacity of certain coatings to protect the Eurofer in much more severe conditions than what will be the working conditions in the breeders. Likewise, the effect of temperature has been studied independently of the action of the pebbles, as well as the effect of the different composition of the pebbles.

2. Materials and methods

The reduced activation stainless steel used in the experiments is Eurofer, and the coatings and pebbles are shown in Table 1. Eurofer samples (7x7x4 mm^3) overcoated on one side were kept in direct contact with the ceramic pebbles for up to 3700 h, in a special cylindrical chamber with a modular design manufactured at CIEMAT in which up to three breeders can be tested simultaneously (It is described in Ref. [8]). Chamber inner walls are covered with ZrO_2 for protection against corrosion, and a stainless steel mesh has been installed between consecutive modules in order to prevent possible breeder mixture as a consequence of the sweep gas. A purge gas flow of ~ 1 cm^3/min is maintained through the different chamber sections, which is controlled by a screw flowmeter. The chamber is introduced in a tubular furnace that permits testing temperatures up to 1500 °C. Corrosion tests have been carried out for two different ceramic pebbles, K-S and J-T at 800 °C for 730 h, and for two different purge gas compositions: He/H_2 (98/2 %vol) and He/H_2O (99.8/0.2 %vol).

The corrosion layer formed after the tests has been studied by scanning electron microscopy/Energy-dispersive X-ray spectroscopy (SEM/EDX) (Zeiss Auriga Compact/Bruker XFlash). A confocal microscopy and interferometry system was used to study the topography of the corrosion layers and obtain 3D images. The equipment used was a Leica DCM8.

3. Results

3.1. Effect of pebbles on corrosion

Fig. 1 shows the corrosion layer that has been produced after a 3700 h test at 550 °C with the pebbles K-S and J-T respectively in He/H_2O flow gas. At the usual working temperature for the pebbles the corrosion layer produced by the K-S pebbles is practically negligible while it is important for the J-T. The reason seems to be the distinct nature of the corrosion layer. While in the case of the K-S corresponds to a vitreous layer composed of silicon, lithium and other metals that adheres and protects the steel, the J-T is oxidic-like and porous, so it does not provide Eurofer with any protection. The exhaustive study of these layers can be found in Ref. [8 and 9]. At higher temperature (800 °C for 730 h), the vitreous silica layer that protects the surface of the Eurofer has disappeared and the corrosion is favored by the small proportion of water contained in the helium purge stream, as can be seen in Fig. 2.

3.2. Effect of the temperature on corrosion

To separate the effect of the temperature itself from that produced in combination with the pebbles, an experiment was carried out in which the temperature was maintained at 800 °C and the time, 730 h, but the pebbles were removed. The results can be seen in Fig. 3.

Generalized corrosion around all material that reaches almost 500 μm depth can be found after the test. The mapping of the elements in the corrosion layer can be seen in Fig. 4. As a consequence of the temperature in a He/H_2O mixture, the corrosion layer is formed by sublayers corresponding to different compositions. Next to the Eurofer is enriched in chromium and slightly in manganese, elements that disappear gradually as the surface approaches. The layer is porous and fragile so it exfoliates easily. Under these conditions, it can be ensured that the adhesion of the layer to the substrate is low and can be detached easily, which means a new exposure of the steel to the medium that will continue to act on it.

Knowing the characteristics of this corrosion layer is important because it constitutes the reference on which the protective capacity of the different coatings exposed below will be compared, as pebbles have little effect at that temperature.

3.3. Effect of coatings

The coatings that have been tested and the manufacturing method are shown in Table 1.

3.4. Thermal projection Al_2O_3 coating

Fig. 5 shows the appearance of the alumina coating prepared by thermal projection before (a) and after (b) the accelerated corrosion test at 800 °C for 730 h with K-S pebbles.

As can be seen in the photographs, the coating remains after an experiment in such severe conditions. The adhesion of this coating is demonstrated in the same way the roughness does not seem to be altered to a great extent. The high temperature and the exposure time of testing are relevant for the beginning of the martensite transformation. Such process involves the movement of the grain boundaries and diffusion of the material towards the pores and manufacturing defects (cracks) of the coating. As seen in Fig. 5 (b) such cavities have been filled with steel, possibly in a mixture of austenite and ferrite. Beyond that part of the steel, the material appears protected.

It is interesting to note that in these conditions the two pebbles produce exactly the same results related to corrosion. This may be due to the fact that the composition no longer influences at this

Table 1
Coatings tested in this work. (**Corrosion test conditions:** 800 °C for 730 h with K-S pebbles).

Coating	Method of preparation	Coating thickness	Coating size	Method description
Al_2O_3	Thermal Projection (TP) [10]	~50 μm	7 × 7 mm	A high-temperature plasma jet generated by arc discharge at high temperature
Al2O3	Pulsed Laser Deposition (PLD) [11,12]	5 μm	7 × 7 mm	Condensation of the plasma atoms on the surface of the substrate.
Nanostructured W	DC magnetron sputtering (MS) [13,14]	3.5 μm	7 × 7 mm	The setup consists of a high vacuum chamber with a base pressure in the 10^{-8} mbar range.
Alcrona (AlCrN)	Arc Evaporation (AE) [15]	2.5 μm	7 × 7 × 4 mm	Arc is struck between the backing plate (anode) and the coating material (cathode)

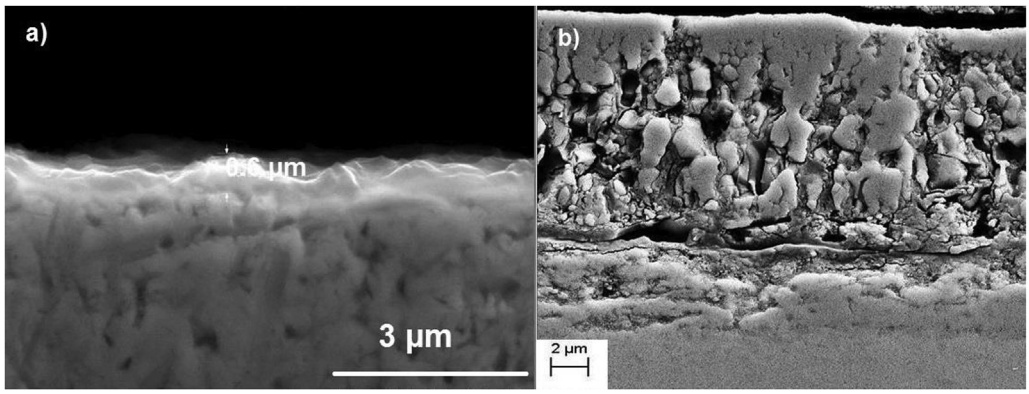

Fig. 1. Corrosion layer produced on Eurofer after 3700 h of exposure to the He/H_2O mixture at 550 °C. a) K-S pebbles. b) J-T pebbles.

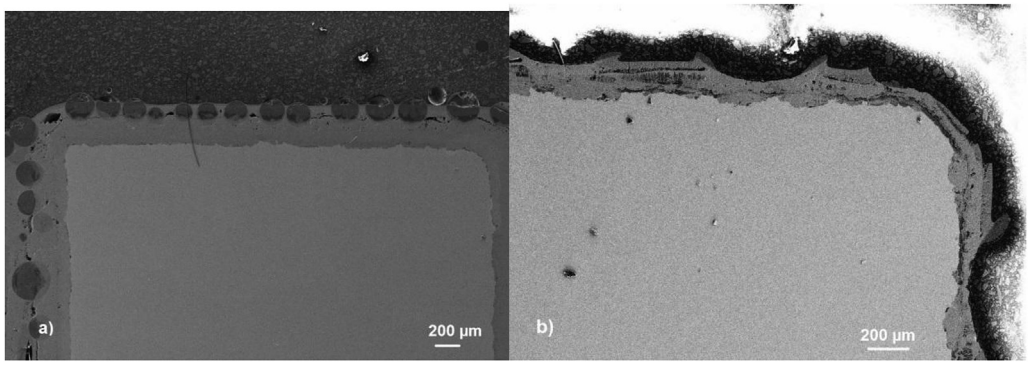

Fig. 2. Corrosion layer produced on Eurofer after 730 h of exposure to the He/H_2O mixture at 800 °C. a) K-S pebbles. b) J-T pebbles.

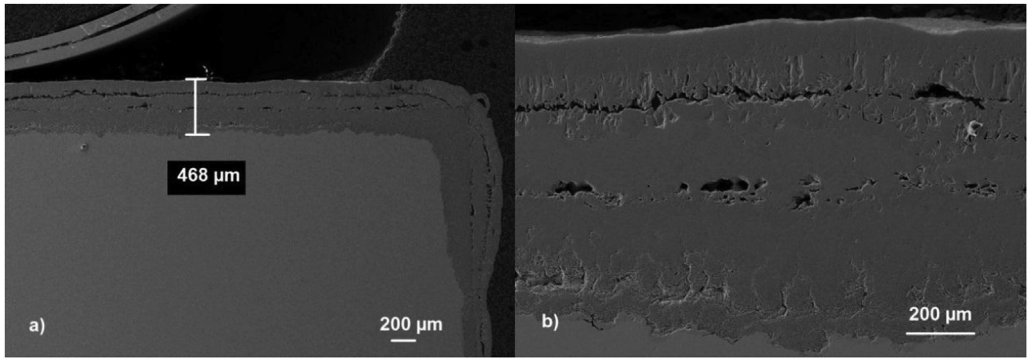

Fig. 3. a) Corrosion layer formed at 800 °C and 730 h without pebbles by the action of a He/H_2O gaseous flow. b) Expanded detail of the layer in which the existence of sublayers is appreciated.

high temperature, as we have seen in the previous section.

3.5. PLD-alumina coatings

Fig. 6a shows the appearance of the coating produced by the PLD technique. As can be seen, it is a homogeneous aluminium oxide layer, well adhered to the substrate and with very low roughness. Fig. 6b shows the confocal image of the coating surface after the corrosion test at 800 °C. As can be seen in the image on the left, the coating is fragmented but remains attached to the substrate. This effect is more perceptible in the 3D image.

The specimen had a prismatic shape in which only one of its faces was covered with aluminium oxide. That face is the one shown in Fig. 7 a) that appears fragmented after the test. It is the huge layer of corrosion that has occurred in another of the faces that had not been protected and in which the K-S pebbles have been immersed. Fig. 7 b) represents a cross section of the probe in which it is possible to distinguish in the upper part the thin layer of alumina that has protected the Eurofer. On the left side and below is the thick layer of corrosion formed as a consequence of the temperature, the pebbles and the atmosphere used in the test.

Facts of special interest are the precipitations observed in the cracks of the coating. The observation by SEM (Fig. 8) shows the precipitation of a phase that forms crystalline sheets. The EDX analysis performed on such structures shows they are formed mostly by oxides of Mn and W, as can be seen in Table 2. To

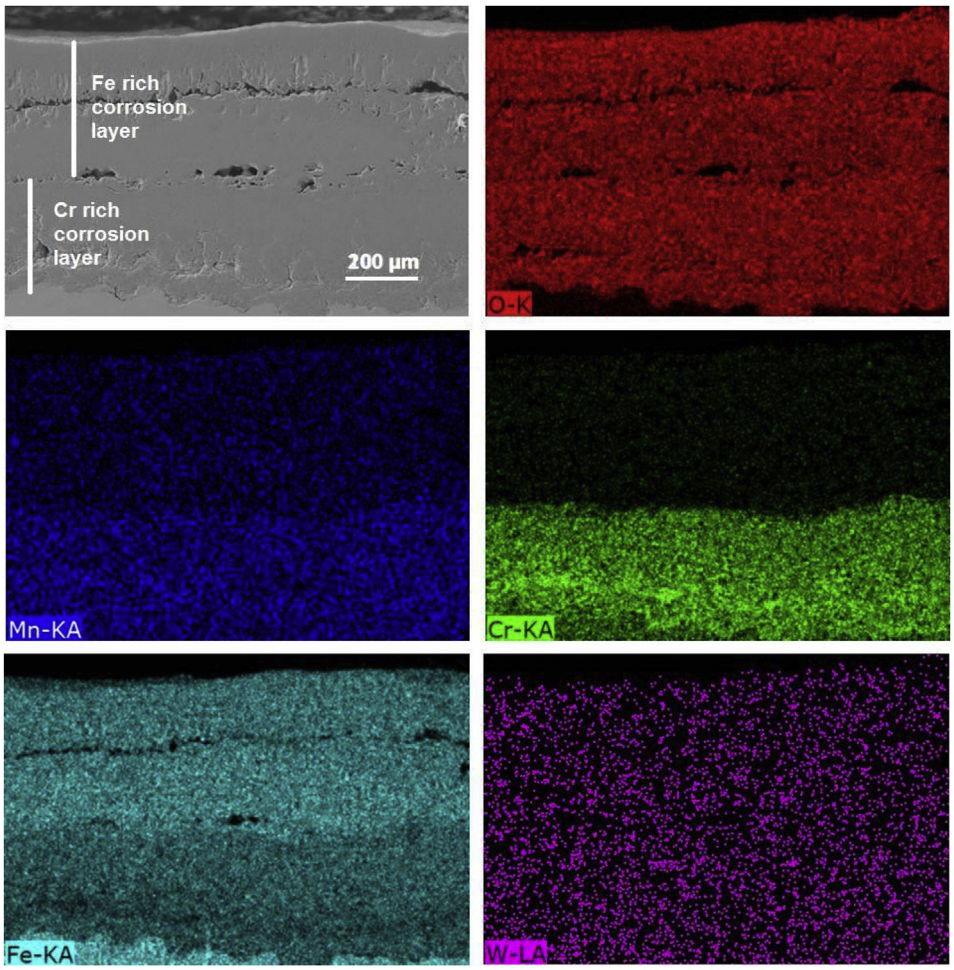

Fig. 4. EDX mapping of the corrosion layer formed on Eurofer steel at 800 °C for 730 h by the action of a He/H_2O gaseous flow without pebbles, showing the composition of the different oxidized sublayers (outer Fe rich and inner Cr rich).

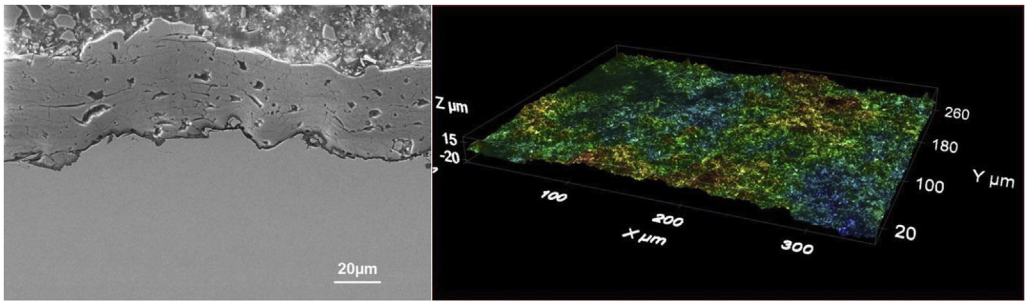

Fig. 5a. Coating prepared by thermal projection "As received". Left: cross section; Right aspect of the roughness obtained by confocal microscopy.

complete the analysis, an EDX was made across one of the excrescences that arise between the fractures of the coating. The analysis does not give rise to doubts of the manganese being involved in its composition.

3.6. Nanostructured W

The case of the nanostructured tungsten coating is very different from alumina. The starting coating appears as a homogeneous layer about 4 µm thick and shows a texture on the surface. The interface is shown without adhesion defects. In this case, the coating was deposited all around the specimen. In Fig. 9 this appearance is described.

Fig. 10 shows the great deterioration suffered by the coating after the corrosion test. At the corrosion test temperature the tungsten layer is not stable and comes off leaving the Eurofer unprotected. Fig. 10 a) presents the final state of the specimen showing it has suffered corrosion on all its faces. The layer formed oscillates between 150 and 200 µm in thickness and, as usual, consists of two sub-layers of different composition. In some areas it is possible to visualize remnants of the original nanostructured W layer between the lithium silicate pebbles (Fig. 10 b). These remains

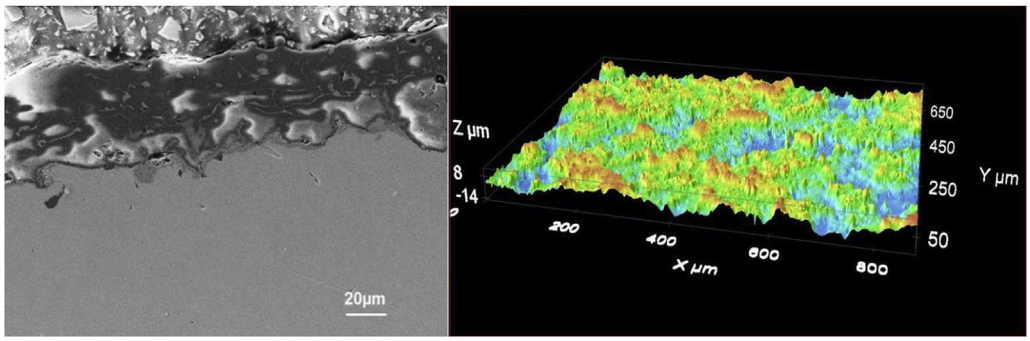

Fig. 5b. Appearance of the TP-coating after the accelerated corrosion test with K-S pebbles and He/H_2O mixture as purge gas at 800 °C for 730h. Left: cross section of the coating. Right: appearance of roughness after the test obtained by confocal microscopy.

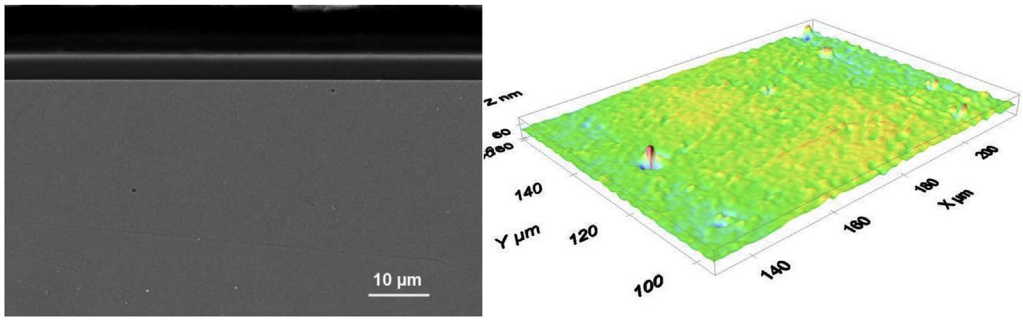

Fig. 6a. SEM cross section and surface of "as received" alumina coating prepared by PLD.

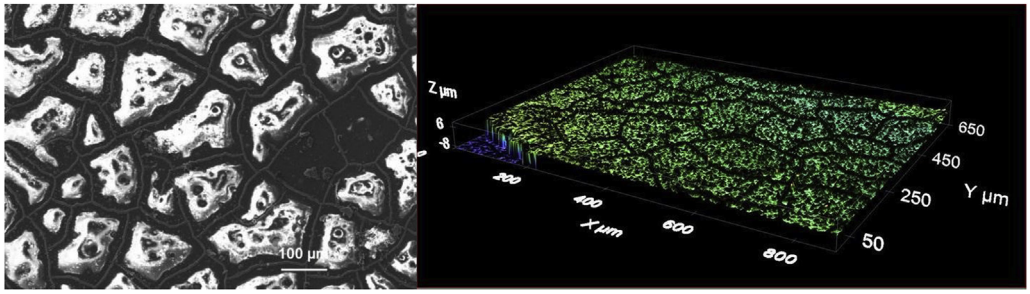

Fig. 6b. SEM planar view and roughness obtained by confocal microscopy of the PLD layer after the corrosion test at 800 °C with K-S pebbles for 730h.

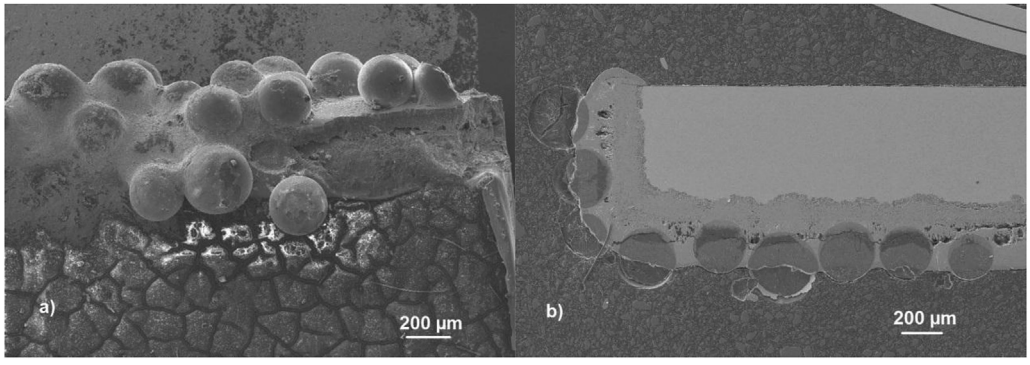

Fig. 7. Coating prepared by PLD after corrosion test at 800 °C with K-S pebbles for 730h. a) SEM front view of the coating after the test. b) SEM cross section.

appear as spherical shapes between frames of acicular crystals. The analysis of the crystals appeared on the surface carried out by EDX shows they are mostly composed of manganese oxide (Fig. 11 and Table 3). As in the case of the PLD-alumina coating, manganese seems to diffuse easily to the surface and form crystalline structures with the silica from the lithium silicate pebbles.

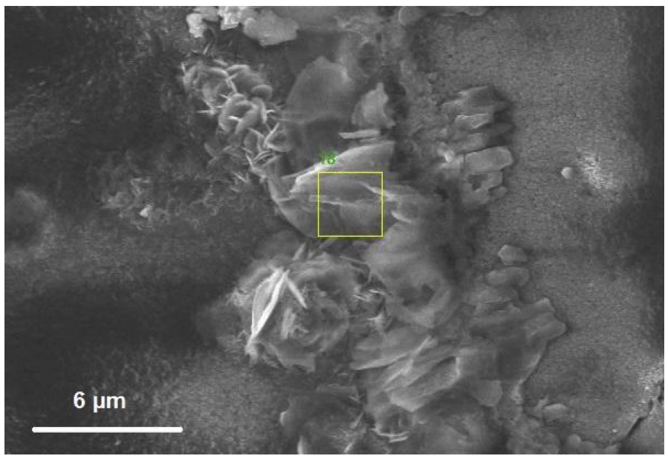

Fig. 8. SEM image of the precipitated crystals found in the cracks of the PLD-coating after the corrosion test at 800 °C with K-S pebbles for 730h, highlighting the EDX analysis area.

Table 2
EDX analysis of precipitated crystals found in the cracks of the PLD-coating after the corrosion tests.

Element	Atomic number	EDX line	Atomic conc. %	Error (1 sigma)
O	8	K	75.36	1.89
Mn	25	K	13.32	0.77
Al	13	K	8.57	0.34
Fe	26	K	1.68	0.12
W	74	L	1.07	0.23

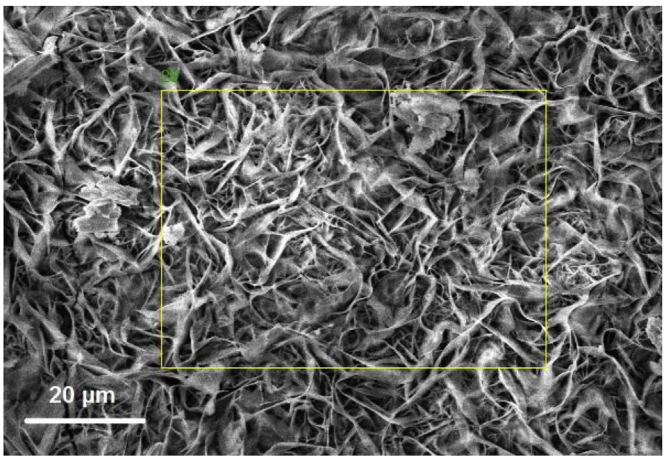

Fig. 11. Surface SEM image of the crystals found on the surface for the nanostructured W coating after corrosion test highlighting the EDX analysis area.

Table 3
EDX analysis of the crystals found on the surface for the nanostructured W coating after corrosion test.

Element	Atomic number	EDX line	Atomic conc. %	Error (1 sigma)
O	8	K	75.80	1.70
Mn	25	K	14.10	0.73
Fe	26	K	8.61	0.46
W	74	L	1.49	0.27

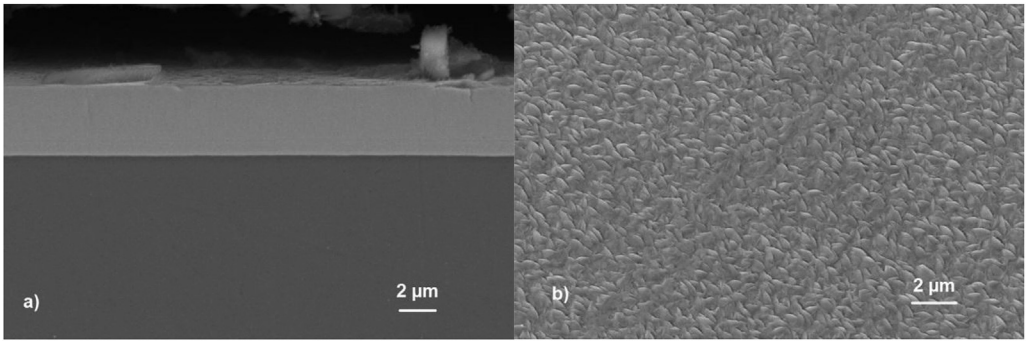

Fig. 9. Cross section view a) and texture b) of "as received" nanostructured W coating.

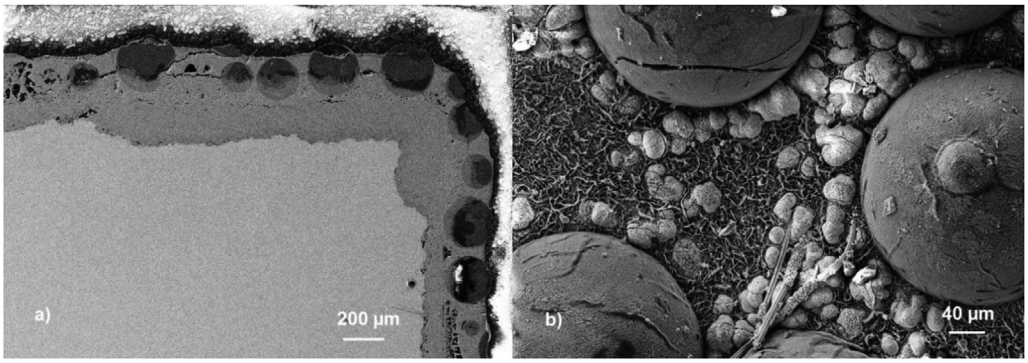

Fig. 10. a) Corrosion layer produced in the nanostructured coating after the corrosion test at 800 °C with K-S pebbles for 730h. b) Remains of the original nanostructured W coating.

3.7. ALCRONA (Al/Cr oxinitride)

Alcrona is a commercial name that corresponds to the composition of a mixed nitrous aluminum and slightly oxidized chromium. The appearance of the "as received" coating is shown in Fig. 12. It is a homogeneous coating although it has variable thicknesses, depending on the area. Similarly, the roughness is not homogeneous either. The compositional profile is shown in Fig. 13.

The situation that arises after the corrosion test at 800 °C is complex. Fig. 14 shows the thick layer of corrosion produced when the Eurofer specimen has been in contact with the K-S pebbles, which approximates 500 μm thick. This result seems to indicate that the ALCRONA layer left the steel uncovered in the first hours of the experiment and did not protect the steel surface at all.

In the EDX analysis of the corrosion layer, traces of the coating are not detected. The layer of oxides formed is what is usually found in these cases, formed by two sublayers of different composition, the closest to the steel being enriched in chromium. Fig. 15 shows the analysis.

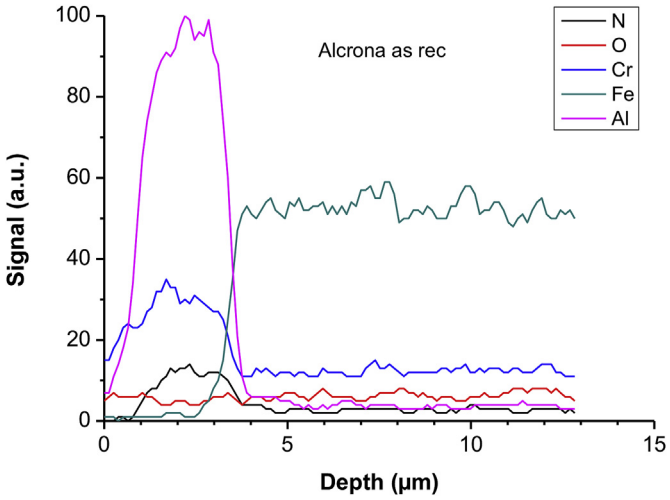

Fig. 13. Cross sectional EDX analysis of the "as received" ALCRONA coating.

4. Discussion

Table 4 summarizes the results regarding the corrosion produced with solid breeders. It is important to note that although only the results obtained with the K-S pebbles have been described, the results are similar for the J-T. When the temperature rises from 550 °C to 800 °C, the differences found at lower temperatures in the corrosion layers disappear, so it is not necessary to repeat comments or pictures. It likely seems that the effect of temperature is more important than that produced by the pebbles and is somehow masked. In any case, the results of this experiment are important because this temperature (800 °C) is well above the expected working temperature range of any breeder concept and therefore, it allows speculating on the usefulness of some coatings. If under these severe conditions they are able to protect the steel, they will most likely do it at lower temperatures. On the other hand, the measurements of the corrosion layer thicknesses obtained with the J-T pebbles can include a major error. Due to the large size of the lithium titanium pebbles they can drag part of the corrosion layer as the remaining pebbles are detached after the test. For this reason, it is more convenient to carry out the discussion based on the corrosions observed with the K-S pebbles.

Thus, before beginning the discussion, it is important to take into account that the thickness of the corrosion layer is not homogeneous and the thickness data shown in Table 4 are calculated on a minimum of 10 different points.

The first result to discuss is the effect of temperature. As seen in Figs. 3 and 4, the corrosion layer formed solely by the action of the purge gas at 800 C is very important. The protective layer that the silicon-containing pebbles form on the Eurofer (an amorphous lithium silicate) that has been discussed in previous papers [8], is not stable at high temperature, so it does not form, or if it forms in a first stage, decomposes and leaves the material completely unprotected to external actions (Fig. 2).

The same happens with some of the commercial coatings tested in this study. The data obtained with respect to ALCRONA commercial coating indicate that it is not stable under the conditions considered and disappeared in the early stages of the test, giving rise to layers of corrosion similar to those of the uncoated material.

On the other hand, the layer thickness found in the nanostructured tungsten coated material seems to indicate that it was maintained at the beginning of the test and was able to partially protect the surface of the steel, however, after some time that has not been determined; its decomposition began, as demonstrated by the remains found by scanning microscopy. Thus, the thickness of the corrosion layer found for the coating of W is half that corresponding to the bare material.

The only coatings presenting good behaviour are those of alumina. In this work, two different aluminas from the structural point of view have been used as coatings. In the first case, (thermal projection) the layer is formed by alpha Al_2O_3 (or corundum) phase, which is the stable at high temperature, while the alumina deposited by the PLD process is mostly amorphous, with small crystalline microdomains [16]. While there is no possibility of transformations in the first one, the second can change its crystalline structure as a consequence of the time elapsed in the high temperature test. The transformation would produce a volume change that would result in micro cracks that would affect the protective action of the coating. In any case, since the tests were

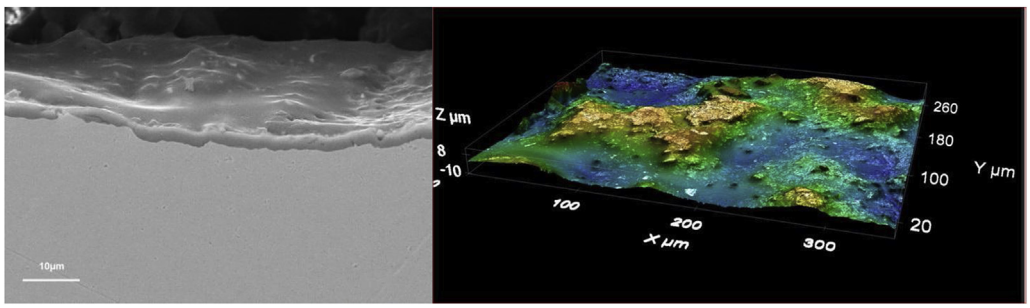

Fig. 12. SEM cross section and roughness of "as received" ALCRONA coating.

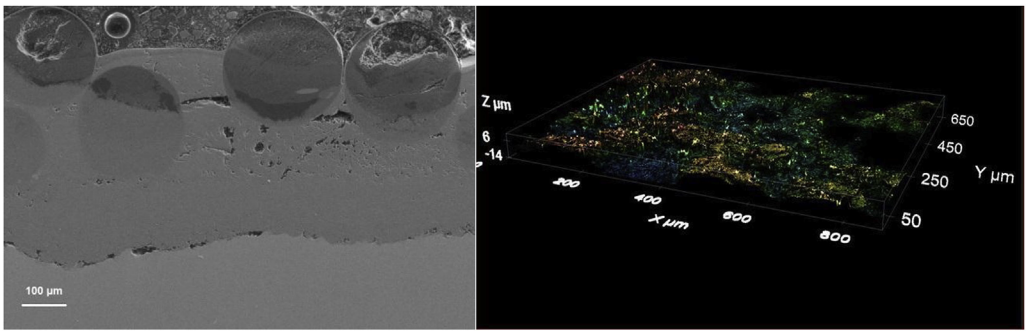

Fig. 14. Corrosion layer produced by the K-S pebbles at 800 °C for 730h in the Eurofer covered by ALCRONA.

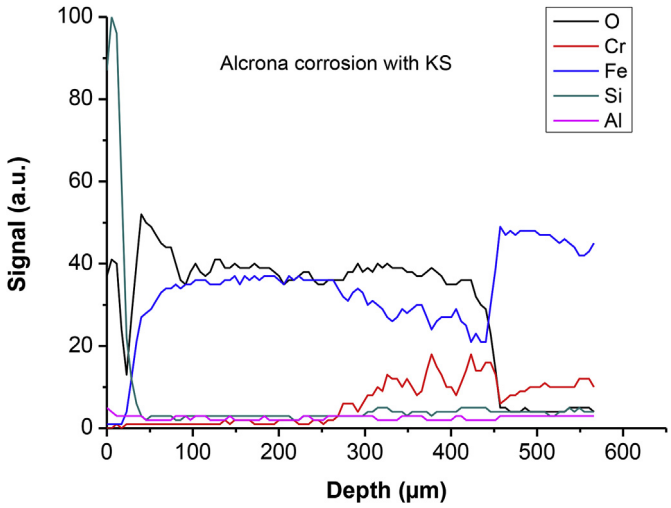

Fig. 15. EDX analysis of the corrosion layer produced on the ALCRONA coating by the K-S pebbles at 800 °C for 730h.

Table 4
Corrosion layer thickness found after corrosion tests.

Coating	800 °C/730h He/H2O		
	K-S (µm)	J-T (µm)	Remarks
Bare/pebbles	460	260	
Bare/without pebbles	–	–	470 µm no pebbles
TP-Al_2O_3	–	–	No corrosion layer observed
PLD- Al_2O_3	–	–	No corrosion layer observed
ALCRONA	480	235	
W	280	180	

carried out in very extreme conditions, it is expected that in the working conditions, this problem does not exist. Although the work times will be significantly greater than in the corrosion test that is presented in the paper, the temperature will not reach that necessary for the transformation of the metastable phases included in the PLD-coating. A layer of dense aluminium oxide, therefore, is established as a good candidate to act both as a barrier to corrosion and to prevent the tritium diffusion [17].

In spite of the results obtained with aluminium oxide coatings, it should be mentioned that there are limitations for using them as a protector in contact with lithium silicates, especially when the purge gas is a He/H_2O mixture. As mentioned above, the pebbles are composed of a mixture of lithium silicates, with the orthosilicate phase being the majority. These species are partially soluble in water and provide an acidic medium. This effect is favoured with the increase in temperature. On the other hand, aluminium oxide coatings can easily react with either a strong base or acid, dissolving in them, and exposing naked Eurofer to the reactive medium. It is for this reason that the use of aluminium oxide as a protector for the HCPB concept can have problems for long working times [18].

5. Conclusions

The work has allowed differentiating between the corrosion due to the temperature and the one due to a combined action with the lithium pebbles. On the other hand, it has been shown that aluminum oxide is an excellent protector even in conditions that far exceeds the working temperature that is expected in the breeder blanket module. The ALCRONA commercial coating is not stable under the test conditions considered and disappeared in the early stages of the test, giving rise to layers of corrosion similar to those of the uncoated material. Finally, nanostructured-Tungsten coating does not seem adequate for 800 °C due to its high volatilization; however, it is expected to work correctly.at lower temperatures (in the range 350ºC-550 °C).

Acknowledgements

The authors wish to thank M. Martín, J.M. García, J. Valle and F.Jiménez for their help in the experiments. Thanks are also due to Oerlikon Balzers Coating Spain S.A.U. and Tratamientos Superficiales Iontech, S.A for providing the authors with ALCRONA and thermal projected alumina layers respectively.

This work has been carried out within the framework of the EUROfusion Consortium and has received funding from the Euratom research and training programme 2014-2018 under grant agreement No 633053, and partially supported by the spanish MEIC Project (Ministerio de Economía, Industria y Competitividad) (ENE2015-70300-C3-1-R) and TechnoFusión Project (S2013/MAE-2745) of the CAM (Comunidad Autónoma Madrid). "The views and opinions expressed herein do not necessarily reflect those of the European Commission".

References

[1] J. Konys, INEPT Nuclear Fuel Training, KIT-CN, 2012. March 5-9.
[2] M. Carmona Gázquez, T. Hernández, F. Muktepavela, E. Platacis, A. Shishko, Magnetic field effect on the corrosion processes at the Eurofer–Pb–17Li flow interface, J. Nucl. Mater. 465 (2015) 633–639.
[3] A.R. Raffray, M. Akiba, V. Chuyanov, L. Giancarli, S. Malang, Breeding blanket concepts for fusion and materials requirements, J. Nucl. Mater. (2002) 307–311, 21–30.
[4] K. Mukai, F.J. Sanchez, T. Hoshino, R. Knitter, Corrosion characteristics of reduced activation ferritic-martensitic steel EUROFER by Li_2TiO_3 with excess Li, Nucl. Mater. Energy 15 (2018) 190–194.
[5] F. Hernández, F. Arbeiter, L.V. Boccaccini, E. Bubelis, V. Chakin, I. Cristescu,

B.E. Ghidersa, M. Gonzalez, W. Hering, T. Hernandez, X.Z. Jin, M. Kamlah, B. Kiss, R. Knitter, M. Kolb, P. Kurinskiy, O. Leys, I. Maione, M. Moscardini, G. Zhou, Overview of the HCPB research activities in EUROfusion, IEEE Trans. Plasma Sci. 46 (6) (2018) 2247–2261.
[6] C. Alvani, J. Avon, S. Casadio, M.A. Fiitterer, M.R. Mancini, C.A. Nannetti, S. Ravel, N. Roux, L. Sedano, V. Violante, A. Terlain, M. Tourasse, S. Tosti, M. Zanotti, Effect of purge gas oxidizing potential on tritium release from Li-ceramics and on its permeation through 316L SS clads under irradiation (TRINE experiment), J. Nucl. Mater. 233–237 (1996) 1441–1445.
[7] T. Hernández, P. Fernández, R. Vila, Corrosion susceptibility of EUROFER97 in lithium ceramics breeders, J. Nucl. Mater. 446 (2014) 117–123.
[8] T. Hernández, M. Carmona Gázquez, F. Sánchez, M. Malo, Corrosion mechanisms of Eurofer produced by lithium ceramics under fusion relevant conditions, Nucl. Mater. Energy 5 (2018) 110–114.
[9] T. Hernández, P. Fernández, Corrosion susceptibility comparison of EUROFER steel in contact two lithium silicate breeders, Fusion Eng. Des. 89 (2014) 1436–1439.
[10] I. Shakhova, E. Mironov, F. Azarmia, A. Safonov, Thermo-electrical properties of the alumina coatings deposited by different thermal spraying technologies, Ceram. Int. 43 (17) (2017) 15392–15401.
[11] Douglas B. Chrisey, Graham K. Hubler (Eds.), Pulsed Laser Deposition of Thin Films, John Wiley & Sons, 1994. ISBN 0-471-59218-8.
[12] F.G. Ferré, M. Ormellese, F. Di Fonzo, M.G. Beghi, Advanced Al_2O_3 coatings for high temperature operation of steels in heavy liquid metals: a preliminary study, Corros. Sci. 77 (2018) 375–378.
[13] K. Ishii, High-rate low kinetic energy gas-flow-sputtering system, J. Vac. Sci. Technol. 7 (1989) 256–258.
[14] N. Gordillo, M. Panizo-Laiz, E. Tejado, I. Fernandez-Martinez, A. Rivera, J.Y. Pastor, C. Gómez de Castro, J. del Rio, J.M. Perlado, R. Gonzalez-Arrabal, Morphological and microstructural characterization of nanostructured pure -phase W coatings on a wide thickness range, Appl. Surf. Sci. 316 (2014) 1–8.
[15] Sablev et al., US Patent #3,793,179, 19 Feb. 1974.
[16] F. Di Fonzo, M. Vanazzi, D. Iadicicco, M. Utili, S. Bassini, M. Tarantino, T. Hernandez, A. Moroño, P. Muñoz, in: Multifunctional Nanoceramic Coatings for Future Generation Nuclear Systems, 30th SOFT Conference, Messina, Sicily, Italy, 2018.
[17] C. Henager, in: Russell H. Jones (Ed.), Hydrogen Permeation Barrier Coatings, Materials for the Hydrogen Economy, George J. Thomas, 2007, pp. 181–190. Edited By.
[18] C. Novák, G. Pokol, V. Izvekov, T. Gál, Studies on the reactions of aluminium oxides and hydroxides, J. Therm. Anal. 36 (5) (1990), 1895–1909.